⌫ Retour au sommaire

2. Czochralski method

The industrial growth of silicon single crystals for electronics is based on the Czochralski pulling technique. Large ingots (ϕ=10 cm, L=90 cm) weight 18 kg.

GaAs, GaP for electronics, $Gd_3Ga_5O_{12}$:Nd^{3+}, $Y_3Al_5O_{12}$:Nd^{3+} (ϕ=5 cm, L=20 cm) for laser applications (and gem imitation), $LiNbO_3$ for optics and fluorides are, or were, produced at a much smaller scale.

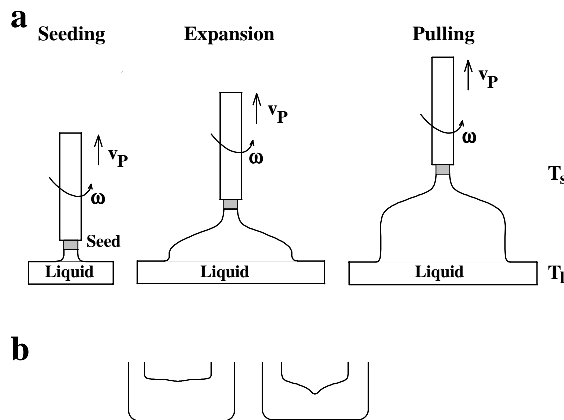

Figure 14. - Successive steps of Czochralski pulling technique.

An oriented crystal seed is fixed (figure 14) at the lower end of a rotating and translating vertical rod (ω rotation and v_P pulling rate or growth speed). It is kept at $T_S<T_m$, brought into contact with the fused melt ($T_l \approx T_m$) and pulled up. The liquid is attracted by capillarity and submitted to the temperature gradient T_S-T_l. The temperature gradient and the pulling rate v_P are then adjusted in order to increase the diameter of the crystallising solid (expansion operation). When the required diameter (≈25-100mm) is obtained, the ω, v_P, T_l, T_S parameters are regulated in order to keep constant the radius (R) or the weight increase of the crystal.

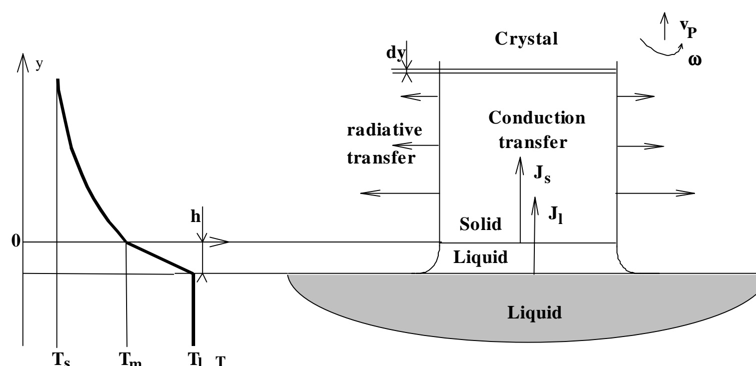

Figure 15. - Idealised temperature profile and heat exchange in Czochralski pulling technique.

Modelisation of the experiment is very complex : radiative (ΔH_{rad}) and non radiative (ΔH_{cond}) heat transfers, mass transport and diffusion, viscosity, gravity, must be taken into account. Consequently, a very simplified (and unphysical) model is given hereafter (figure 15), in order to estimate the influence of the experimental parameters. A linear temperature gradient, along y, is supposed to establish in the

liquid film attracted by capillarity (height h). The liquid-solid interface is supposed to be planar. At this interface ($y = 0,\ T = T_m$), the heat exchange, during the unit time, is :

$$\left|\vec{J}_s - \vec{J}_l\right| S = v_p \rho S \Delta H_m \quad \text{or} \quad \chi_s \left[\left(\frac{\partial T}{\partial y}\right)_{y=0}\right] - \chi_l \left(\frac{T_l - T_m}{h}\right) = v_P \rho \Delta H_m \qquad \{12\}$$

In the solid, in steady-state conditions, summation of radiative (ΔH_{rad}) and conductive (ΔH_{cond}) heat fluxes through a closed surface Σ is nul. The surface is limited here by the cylinder of height dy and radius R (figure 15), σ is the emissivity and ε is the Stephan's constant.

$$\sum \Delta H = 0 = \Delta H_{rad} + \Delta H_{cond} \qquad \{13\}$$

$$= -\sigma\varepsilon T^4 dS - \vec{J} d\vec{\Sigma} = -\sigma\varepsilon T^4 dS - \mathrm{div}\vec{J} dv$$

$$= -\sigma\varepsilon T^4 (2\pi R dy) + \chi_s \pi R^2 dy \nabla^2 (T)$$

hence, $$\frac{\partial^2 T}{\partial y^2} = 2\frac{\sigma\varepsilon}{\chi_s R} T^4 \qquad \{14\}$$

If the crystal growth of metals (Si ...) is considered, the thermal conductivity is approximated by : $\chi_s = \chi_m \dfrac{T}{T_m}$, then : $\dfrac{\partial^2 T}{\partial y^2} - 2aT^3 = 0$, with $a = \dfrac{\sigma\varepsilon T_m}{\chi_m R}$.

A solution of this partial differential equation is : $T = \dfrac{A}{1 + By}$.

The limit conditions ($T = T_m$ at $y = 0$ and $\dfrac{\partial T}{\partial y} = 0$ at $y = \infty$) give :

$$T = \frac{T_m}{1 + a^{1/2} T_m y} \quad \text{and} \quad \left(\frac{\partial T}{\partial y}\right)_{y=0} = -\frac{1}{\sqrt{R}} \left(\frac{\sigma\varepsilon}{\chi_m}\right)^{1/2} T_m^{5/2} \qquad \{15\}$$

Replacing in equation 12 finally leads to :

$$\frac{1}{\sqrt{R}} (\sigma\varepsilon\chi_m)^{1/2} T_m^{5/2} = v_P \rho \Delta H_m + \chi_l \left(\frac{T_l - T_m}{h}\right) \qquad \{16\}$$

This expression shows that the radius of the cylindrical crystal decreases when T_1, v_P or ω increase (h decreases) ; this radius is approximately proportional to $\omega^{-1/2}$. It must be noted that the preceding hypotheses rarely hold. Moreover, a flat interface does not necesseraly favour the crystal quality (bubble trapping occurs). A convex interface is preferred (figure 14) and its shape depends strongly on the ω rotation speed.

Impurity segregation is calculated by considering the amount of impurity B which is rejected in the liquid during crystallisation. The solidified fraction g is defined by $g = m_s / M$ (crystal/total mass ratio)

$$(C_B^l - C_B^s) dm = m_l dC_B^l \quad \Rightarrow \quad \frac{dC_B^l}{C_B^l - C_B^s} = \frac{dm}{m_l} = \frac{Mdg}{M(1-g)}$$

Integration gives : $C_B^l = \frac{C_0}{(1-g)^{1-k}}$ and $C_B^s = \frac{kC_0}{(1-g)^{1-k}}$ {17}

The relative concentration C_B^s/C_0 is presented in figure 16 for k=0.1 and compared with zone melting $(1/L = 1/20)$ for a single pass.

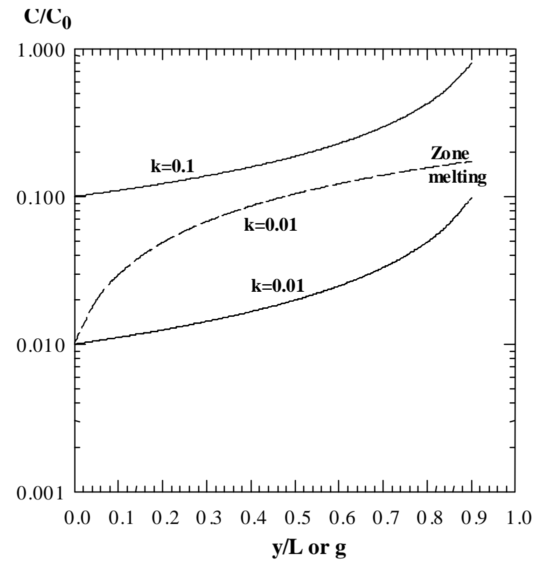

Figure 16.
Impurity concentration in a crystal obtained by Czochralski pulling technique compared with fusion zone melting.

Materials which have been obtained by Czochralski growth include :

- semiconductors (Si (T_m=1420°C), GaAs (T_m=1283 °C) or GaP (T_m=1468 °C at P_{eq}=3.8 MPa)),
- cubic garnets ($Gd_3Ga_5O_{12}$ (GGG) T_m=1730 °C ; $Nd_3Ga_5O_{12}$ T_m=1515 °C ; $Sm_3Ga_5O_{12}$ T_m=1620°C)), $LiNbO_3$ (T_m=1980 °C),
- cubic perovskite fluorides ($RbCaF_3$ T_m=1120 °C ; $KZnF_3$ T_m=870 °C),
- layered perovskites $K_xRb_{1-x}AlF_4$ (T_m=550 °C),
- laser materials ($LiCaAlF_6:Cr^{3+}$ (T_m=825 °C)), $SrAlF_5$ (T_m=887 °C), $BaMgF_4$ (T_m=940 °C).

It must be noted that most of these phases do not melt congruently for the stoechiometric ratios indicated above. Frequently, one of the constituents presents a non negligible pressure and partially evaporates at the growth temperature : P or As in III-V semiconductors, ZnF_2 in fluorides, Ga_2O_3 in GGG (the congruent melting phase is $Gd_{3.05}Ga_{4.95}O_{12}$).

For GaP, the dissociation reaction is : $GaP \rightarrow Ga + \frac{1}{n}P_n$

The stabilization of GaP for crystal growth is achieved by one of the following solutions :

- compensation of the partial pressure of phosphorus ; the crystal and the melt are encapsulated in fused B_2O_3 ($T_{softening}$=425 °C) and heated in a high pressure equipment in order to keep P_{eq}>3.8 MPa ;
- decrease of the temperature and of the phosphorus fugacity in the melt by starting from a 5 % or 10 % phosphorus concentration (figure 17) ; the temperature must be lowered during crystal growth along the liquidus curve BA.

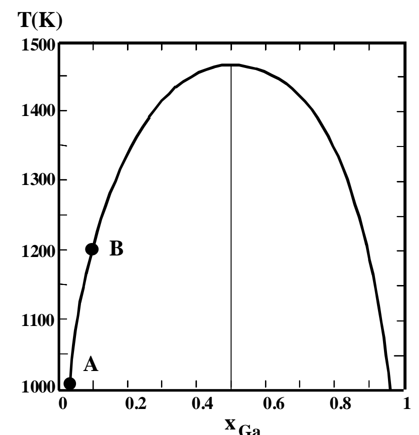

Figure 17. - Ga-P phase diagram.

The control of the temperature allows for the extension of Czochralski growth to incongruently melting phases. This is illustrated by the growth of $BaLiF_3$ (inverse perovskite with Li in octahedral coordination, T_m=826 °C). The LiF-BaF_2 phase diagram is given in figure 4.a. It shows that $BaLiF_3$ crystallises from a LiF rich liquid (B composition). The temperature must be lowered during crystallisation at a speed which depends on the weight of the crystal. The BA liquidus curve is first computed from equation 2 with ΔH_f=45kJ.mole^{-1}. Then, the variation of the temperature with time is calculated for the initial charge of melt (260 g, 43 % BaF_2 - 57 % LiF) and for the crystallisation conditions (v_P=1 mm/h, crystal diameter ϕ=30 mm). The theoretical variation dT/dt is shown in figure 18 together with the experimental temperature program.

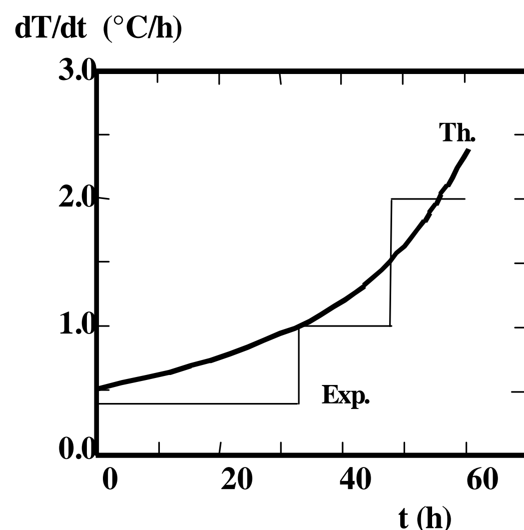

Figure 18.
Temperature variation for the crystal growth of incongruent melting $BaLiF_3$.

Solid solutions $(Ba_{1-x}Pb_x)LiF_3$ were also investigated and lead was analysed for several positions along the generatrix of the crystals. Lead concentration was then deduced as a function of the solidified fraction g. The segregation coefficient for Pb^{2+} in $BaLiF_3$ is k≈0.05, as obtained from the fit of equation 17.

Other incongruently melting phases, grown by Czochralski technique can be cited : $LiYF_4$ (T=815 °C), K_2CoF_4 (T=830 °C). Several examples are listed in table 2.

Table 2 : Examples of materials obtained by Czochralski growth.

	Material	Structure type	(Solvent)	Temperature (range) (°C)	Cooling rate (°C/h)	Rotation ω (rpm)	Translation v_P (mm/h)
Oxides	$Y_3Al_5O_{12}$	Garnet	$BaO-B_2O_3$	1350-1250		60	0.2
	$Bi_{12}SiO_{20}$	Eulytite	$6Bi_2O_3$ SiO_2	900		20	0.35
Fluorides	YF_3		$0.8YF_3$-0.2LiF	1050-850		30	1
	$LiYF_4$	Scheelite	0.51LiF-$0.49YF_3$	815-695		10	2.5
	$KZnF_3$	Perovskite	$KZnF_3$	870		20	1
	$BaLiF_3$	Perovskite	$0.43BaF_2$-0.57LiF	830-780	0.5,1,2	10	1
	$BaMnF_4$		$BaMnF_4$	755		20	4
	K_2ZnF_4		$0.3ZnF_2$-0.7KF	720-675	5	60	10